



PERGAMON

Available online at www.sciencedirect.com

SCIENCE @ DIRECT®

Applied Radiation and Isotopes 58 (2003) 333–338

Applied
Radiation and
Isotopes

www.elsevier.com/locate/apradiso

Study of air pollutants in Hong Kong using energy dispersive X-ray fluorescence

A.K.M. Chu^a, H.H. Cheng^a, R.C.W. Kwok^b, K.N. Yu^{a,*}

^aDepartment of Physics and Materials Science, City University of Hong Kong, Tat Chee Avenue, Kowloon Tong, Kowloon, Hong Kong

^bDepartment of Public and Social Administration, City University of Hong Kong, Tat Chee Avenue, Kowloon Tong, Kowloon, Hong Kong

Received 21 August 2002; received in revised form 15 October 2002; accepted 2 December 2002

Abstract

Airborne particulate samples were collected from various reference sites in Hong Kong and the energy dispersive X-ray fluorescence (EDXRF) intensities for 19 chemical elements were recorded. Principal component analysis (PCA) was employed so that the variances of these 19 original variables were captured by a few new indices called principal components or PCs. Data points for similar sources were automatically grouped together in a plot of the first three PCs (PC plot). Data for the monitoring site Mong Kok were located within the area defined by vehicular emissions. As such, the main air pollutant at this site was concluded to originate from vehicular emissions. A fraction of data for the Causeway Bay monitoring site also fell into this same identified area, so the main air pollutant could also be vehicular emissions. Some of the data located either on or outside the border can be explained in terms of meteorology.

© 2003 Elsevier Science Ltd. All rights reserved.

Keywords: Energy dispersive X-ray fluorescence; Principal component analysis; PCA; Air pollutants

1. Introduction

Notwithstanding the identifications of high concentrations of anthropogenic aerosols in Hong Kong, few studies have been made on the source of these aerosols. Total suspended particulates (TSP) were sampled in the western part of the New Territories between 1986 and 1987 (Fung and Wong, 1995); the study involved various trace elements (e.g., Se, As, Sr, V, etc.) as markers. More recently, compositional data in the period 1992–1996 (Hong Kong Environmental Protection Department, 1997) were used with the positive matrix factorization method to identify nine sources for the air pollutants in Hong Kong (Lee et al., 1999).

Despite these findings and despite growing concern about air pollution in Hong Kong, controversies remain over prime air pollutant sources in various highly

polluted areas. For example, while some believe that the main air pollutant in Causeway Bay (a well-known highly polluted area in Hong Kong) results from vehicles, others believe the main pollutants to be non-vehicular, coming from coal-fired power plants or from cross-border pollutants trapped in Causeway Bay, the area being situated in front of high mountains. Chemical mass balance is conventionally the most appropriate method used for this kind of source apportionment, but the crucial step in this is determination of the composition of material emitted by a variety of local air pollution sources (or source profiles). While by definition source profiles are specific to a site, very few source profiles for different air pollutant sources have been determined for Hong Kong (Yu et al., 2002, Yeung et al., 2003). To this extent, sources of air pollutants in Hong Kong cannot as yet be identified through the chemical mass balance method. The objective of the present work is to devise a method for identifying the main sources of air pollutants in an area without having to determine the corresponding source profiles.

*Corresponding author. Tel.: +852-2788-7812; fax: +852-2788-7830.

E-mail address: peter.yu@cityu.edu.hk (K.N. Yu).

2. Methodology

The principal component analysis (PCA) technique (e.g., Manly, 1986, Stephenson and Radmore, 1990) will be employed for our present task. The PCA employs new indices called principal components or PCs to capture the variances of the original variables (i.e., the variation of the original data). The first new index will capture the largest possible variances from the original variables, the second will capture the largest possible variances left over from this process, and so on. In other words, consecutive indices are extracted in a way which maximizes the variability not captured by the preceding index. If most of the variances of the original variables can be captured by the first few PCs, the variation in the original data set can be adequately described by these few PCs.

Different categories of data having different distributions of elemental abundance will give different values for the PCs, and the reduced number of indices can be plotted in 2D or 3D plots for a visually comprehensible identification of clustering of data (Kendall, 1980). Such 2D and 3D plots of PCs have been used in a number of fields of research where data classification has been required. For example, these have been used extensively in studies of the provenance and dating of ancient Chinese porcelains by Yu and Miao (1996, 1997). PCA has also been applied in microanalysis of individual aerosol particles (Orlic, 1995). In the present work, 3D plots of PCs will be exploited to identify the main air pollutants in a locality, also avoiding a need to determine the corresponding source profiles.

Ambient particulate samples were collected from September 2000 to March 2001 at 14 reference sites and 2 monitoring sites in Hong Kong. Among the 14 reference sites, 5 were primarily subjected to vehicular emissions (including 3 covered bus terminals and 2 covered car parks, hereafter referred to as VE sites); 8 were primarily subjected to aerosol sources other than vehicular emissions (including 1 construction site, 3 industrial sites, 2 sites near power plants and 2 sea coast sites, hereafter referred to as non-VE sites); and 1 was a hybrid-source site (an industrial site with a bus stop and two petroleum stations nearby, hereafter referred to as the H site). The two monitoring sites were chosen to be Mong Kok and Causeway Bay, each of which are well-known to suffer severe air pollution.

Our objective was to demonstrate, by the method depicted above, identification of the main source of air pollutants at these two sites. A total of 27 samples from the 14 reference sites and 15 samples from the 2 monitoring sites (8 for Mong Kok and 7 for Causeway Bay) were collected on different days.

Each TSP sample was collected using a glass fiber filter (TFAGF41, from Staplex, New York) at 1 m above ground using a dc pump (2032-101-G616X, from Gast

Table 1

Combinations of EDXRF parameters and X-ray filters employed for the different studied chemical elements

Elements	Voltage (kV)	Current (μ A)	X-ray filter
Na, Mg, Al, Si	10	500	nil
S, Cl	15	250	nil
V, Cr, Mn, Fe,	25	120	nil
Cd, K, Ca	40	500	Cu
Ni, Cu, Zn, As, Pb, Br	50	500	Mo

Manufacturing, Inc., Michigan) for 1 h with a flow rate at $2.4 \text{ m}^3 \text{ h}^{-1}$ or 40 l min^{-1} . The filter samples were sealed in separate clean polyethylene bags for return to the laboratory for energy dispersive X-ray fluorescence (EDXRF) analyses. Only EDXRF intensities (in count/s) of the studied metals were employed in the present study. The PCA results would be the same even if we took extra calibration steps to convert the EDXRF intensities into airborne concentrations for the chemical elements, since only the standardized parameters (i.e., deviations from the means in terms of number of standard deviations) are utilized in the PCA. The 19 studied species were Na, Mg, Al, Si, S, Cl, Cd, K, Ca, V, Cr, Mn, Fe, Ni, Cu, Zn, As, Pb, Br. In order to maximize the EDXRF sensitivities for the wide range of elements in which we have interest, five different combinations of EDXRF parameters (including voltage and current) and X-ray filters were employed for different metals for a single air filter sample, as shown in Table 1. The EDXRF $K\alpha$ line intensities were measured for all elements except Cd and Pb, for which the $L\alpha$ line intensities were measured. For better efficiencies, the applied voltage increased in general with the required $K\alpha$ or $L\alpha$ line energies. The current was adjusted to maintain similar live detection time percentages. X-ray filters were used for particular line energies in order to reduce corresponding background intensities. After subtraction of the blank-filter spectrum from that of a sample, we obtained the net intensities of elements for the given sample. The net intensities of these 19 chemical elements then became the 19 original variables for the subsequent PCA.

3. Results and discussion

The EDXRF $K\alpha$ line intensities for all elements except Cd and Pb, and the $L\alpha$ line intensities for Cd and Pb of all our 42 samples are shown in Table 2.

The PCA for our data gave five PCs whose eigenvalues (equivalent to the variances of the corresponding PCs, see above) are greater than one. In

Table 2

Intensities (count/s) of elements of all 42 samples. The EDXRF K α line intensities were measured for all elements except Cd and Pb for which the L α line intensities were measured. (Δ): Lamma Island coal-fired power plant (data encircled by the dotted line); (+): Coastal areas (data encircled by the dash-dotted line); (*): construction sites; (\times): industrial sites; (∇): Lung Kwu Tan coal-fired power plant; (\circ): Covered bus terminals; (\square): Covered car parks. (\blacklozenge): Mong Kok; (\bullet): Causeway Bay; (\ominus): H site; Dashed line: encircling the data points of VE sites, the H site and the two monitoring sites

Site	Na	Mg	Al	Si	S	Cl	Cd	K	Ca	V	Cr	Mn	Fe	Ni	Cu	Zn	As	Pb	Br
\circ	0.35	0.05	0	0	103.7	3.67	1.96	2.96	2.63	0.95	1.36	2.09	5.54	0.67	0.37	1.07	0.73	0.74	0.49
\circ	0.95	0.78	0.01	0.03	109.6	4.69	3.16	5.49	6.04	1.26	1.05	1.90	12.29	0.93	0.75	1.67	1.13	1.10	0.42
\circ	1.89	1.64	0	0	28.7	28.02	9.56	10.87	12.77	3.96	4.75	4.02	27.92	0.48	0.15	0.92	1.42	1.40	0.67
\circ	0.59	0	0	0	6.8	8.79	11.68	14.20	184.85	0.55	0.37	0.77	6.96	0.46	0.17	0.86	0.64	0.63	0.19
\circ	1.24	1.52	0.26	3.99	90.1	8.55	0	0	0	5.08	7.40	7.21	23.94	0.55	0.12	1.83	1.25	1.22	2.27
*	1.47	0.52	3.61	11.68	115.9	12.27	5.74	8.79	12.99	0.75	0.71	1.58	9.30	0.92	0.58	1.90	1.94	1.92	1.43
*	0.94	0.36	0	0	37.0	7.20	0	0	0	1.12	0.68	1.92	28.77	0.75	0.33	10.41	0.95	0.93	0.19
*	0	0	0	0	69.9	2.66	0	0	0	0.43	0.20	0.62	4.90	0.28	0.10	0.56	0.33	0.32	0.23
\times	1.17	1.25	7.12	42.78	69.1	3.21	8.80	8.95	10.61	1.94	2.18	2.31	9.10	1.75	1.23	2.66	2.81	2.77	2.57
\times	1.31	0.27	0.87	9.21	4.9	4.00	8.04	8.46	3.55	0.39	0.16	0.74	8.35	1.89	1.49	4.86	3.07	3.05	2.27
\times	0.70	0.24	0.69	4.37	18.9	5.48	3.21	5.54	4.52	1.54	1.19	1.34	13.72	0.51	0.33	1.76	1.57	1.53	1.02
\times	0.78	0.46	5.04	42.62	90.6	2.17	0	0	0	0.67	1.13	1.27	3.32	0.10	0.19	0.21	0.14	0.13	0.13
\ominus	1.29	1.22	0	0	162.3	15.96	0	0	0	3.70	5.21	5.49	43.45	0.44	0.08	1.09	0.85	0.82	0.81
∇	0.17	0.01	0	0	4.8	10.55	4.35	6.41	11.61	0.89	1.03	1.39	5.25	0.99	0.51	1.30	1.03	0.97	0.57
∇	0.57	0.08	0	0	135.8	3.95	4.94	7.63	14.73	1.40	1.52	2.43	10.46	0.62	0.49	1.11	1.29	1.28	0.88
Δ	1.23	1.55	2.92	33.25	31.9	2.31	2.55	3.17	3.72	0.06	0.04	0.49	0.58	0.80	0.33	1.41	0.80	0.80	0.40
Δ	1.17	1.99	5.73	37.41	107.9	6.99	2.44	2.41	10.25	1.70	1.66	1.55	4.72	0.63	0.34	1.11	1.22	1.22	0.61
Δ	1.33	3.07	3.21	10.37	29.7	5.22	2.45	2.66	9.34	3.61	5.53	3.11	12.87	0.43	0.11	0.40	0.77	0.74	0.98
+	0.55	0.50	0.85	0.91	129.6	2.60	4.07	3.70	3.21	1.26	1.24	1.66	1.51	0.91	0.40	1.04	1.45	1.42	0.78
+	0.68	0.10	4.70	15.81	3.0	2.49	3.47	4.51	1.89	0.97	1.01	0.99	0.91	0.83	0.53	0.97	1.49	1.48	1.30
+	0.95	0.67	7.97	60.47	6.7	4.14	14.21	13.77	18.17	1.28	2.36	1.97	3.38	2.80	1.80	2.60	4.45	4.43	3.71
\square	0.28	0.34	0.62	0	56.1	6.62	1.18	3.49	31.23	4.39	6.00	3.42	17.36	0.21	0.16	1.26	0.57	0.56	0.23
\square	1.68	1.34	0	0	161.3	11.75	0	0	0	2.91	5.01	4.27	14.32	0.36	0.05	0.68	0.74	0.73	0.84
\square	1.34	2.33	3.59	11.88	113.8	7.77	0	0	0	3.32	5.68	4.36	21.07	0.37	0	2.37	1.05	1.04	0.79
\square	0.30	0.67	0	0	64.7	9.21	2.96	4.30	10.89	4.03	6.00	4.29	15.71	0.54	0.11	1.73	0.93	0.92	0.99
\square	1.11	0.52	0.37	9.40	72.1	3.10	0	0	0	0.96	0.91	1.04	7.18	0.20	0.42	0.69	0.14	0.13	0.10
\square	0.76	0.77	0	0	130.4	5.69	127.81	5.76	9.25	2.35	5.59	2.20	0	1.57	0.79	3.65	1.95	1.94	1.09
\blacklozenge	1.57	1.12	5.08	30.97	5.1	14.45	0.03	0.77	14.35	3.19	5.25	4.17	19.26	3.90	0.31	1.59	1.17	1.15	1.48
\blacklozenge	3.37	1.79	5.75	26.22	41.3	14.45	1.23	3.55	14.89	5.67	7.16	5.05	17.13	0.45	0.16	0.87	0.75	0.75	1.34
\blacklozenge	0.88	1.08	0	0	97.1	14.17	3.79	6.45	17.51	3.43	4.37	4.43	21.64	0.81	0.11	1.07	1.21	1.19	1.53
\blacklozenge	0.22	0.18	0	0	117.7	16.83	2.38	3.70	19.84	4.11	5.38	4.43	15.73	0.71	0.12	0.97	0.99	0.97	1.39
\blacklozenge	0.24	0.22	0	0	138.5	13.10	5.54	7.72	23.30	3.08	3.54	4.67	28.34	0.60	0.20	2.30	1.38	1.32	1.66
\blacklozenge	0.39	1.03	0	0	50.5	13.76	3.79	5.08	19.19	3.37	5.44	3.07	17.15	0.62	0.21	2.40	1.34	1.30	2.06
\blacklozenge	1.68	1.14	1.20	0.71	0	14.45	0.73	3.10	5.38	1.74	2.10	1.91	11.13	0.50	0.80	1.36	0.95	0.93	0.91
\blacklozenge	0.65	0.80	3.32	14.80	0.5	14.45	0	0	4.21	1.44	2.27	2.86	19.03	0.80	0.56	2.15	1.58	1.56	1.48
\bullet	0	0	0	0	6.1	7.35	5.69	3.19	0	1.48	1.50	2.21	17.63	2.52	1.95	6.77	3.43	3.39	2.26
\bullet	3.27	2.50	5.71	36.83	1.4	11.02	10.41	12.05	16.21	2.62	3.74	2.79	28.50	2.55	2.13	3.26	4.23	4.23	4.62
\bullet	3.92	2.12	7.98	43.24	78.0	11.03	3.59	5.35	13.04	3.54	6.44	3.47	16.36	1.12	0.38	33.08	2.24	2.25	3.37
\bullet	3.34	0.31	0	0	62.0	13.37	4.00	5.99	22.49	3.78	4.41	5.03	41.67	0.35	0.04	0.08	0.61	0.60	0.87
\bullet	2.80	1.85	5.30	33.10	80.5	9.50	0.30	1.61	9.35	7.15	6.37	4.95	20.95	0.56	0.87	1.61	1.05	1.04	1.59
\bullet	4.12	3.03	18.28	85.32	60.1	14.35	0.52	5.06	16.55	7.26	0.40	5.93	39.68	0.59	1.11	2.17	1.61	1.59	2.09
\bullet	0.71	0.25	0	0	95.1	10.13	3.98	6.32	5.38	0.98	0.83	1.90	15.75	0.80	0.58	2.50	1.34	1.30	1.21

normal factor analysis, only PCs with eigenvalues greater than one are retained, this being referred to as the Kaiser criterion. Table 3 shows the information obtained for the first five PCs, including the eigenvalues and the corresponding cumulative variance. For visual comprehension purposes, only the 3D plot showing the relationship between the first PC (PC1), second PC (PC2) and the third PC (PC3) is presented (Fig. 1).

While other combinations of PCs have also been plotted, the one described above revealed the clearest structure of the data and was therefore identified for use in our analyses.

The PC plot in Fig. 1 indicates that data points of similar sources are grouped together. For example, the coastal sites, which represent one well-delineated category (data encircled by the dash-dotted line in Fig. 1),

are quite clearly dominated by marine aerosols. The measurements made near the Lung Kwu Tan coal-fired power plant characterize emissions from the power plant since the sampling point was at a position close to (~ 100 m) the stack; the altitude of the sampling point is similar to the height of the stack. Conversely, measurements made near the Lamma Island coal-fired power plant (data encircled by the dotted line in Fig. 1) may not characterize emissions from the power plant; the sampling point being ~ 600 m from the stack (the height of which was 215 m) with the net result that less than 1% of the Gaussian plume will impact the ground at this distance. As such, the areas defined by the data for the two power-plant sites are different, indicating that different pollutants were being sampled. If the data

points for the site near the Lamma Island power plant are in fact not characteristic of the plant itself, they should be similar to data points from sea coast sites, particularly since there is no traffic on Lamma Island. The data points can then be joined with the existing sea-coast data to form a larger coastal area in the PC plot.

Distinct from the above, data points for the VE sites (covered bus terminals and covered car parks) assemble into a single category (data encircled by the dashed line in Fig. 1). It is noted that the source profiles for idling and moving vehicles might be different. Within the covered bus terminals and car parks, both moving and idling vehicles are prevalent. At outdoor sites like the monitoring sites in the present study, where there are plenty of traffic lights, and where slow traffic and traffic jams are frequently encountered, the proportion of driving and idling cars might not be very different from the above situations. It is also noted that the differences between moving and idling vehicles usually fail to show up or are seldom considered in normal practices like CMB or traditional factor analysis.

In effect, the VE sites and non-VE sites were observed to be automatically and unambiguously separated by the PC plot. As such, by obtaining EDXRF intensities for the 19 chosen elements for any particular site in Hong Kong, we can immediately locate the outcome on a PC plot and decide on this basis that the main air pollutant is vehicular emissions, marine aerosol or a coal-fired power plant.

Table 3

The first five principal components (with eigenvalues greater than one) obtained from the 19 selected chemical elements, and the corresponding cumulative variance

Principal component	Eigenvalue	Cumulative variance (%)
1	6.43	33.9
2	4.21	56.0
3	2.12	67.2
4	1.61	75.7
5	1.33	82.7

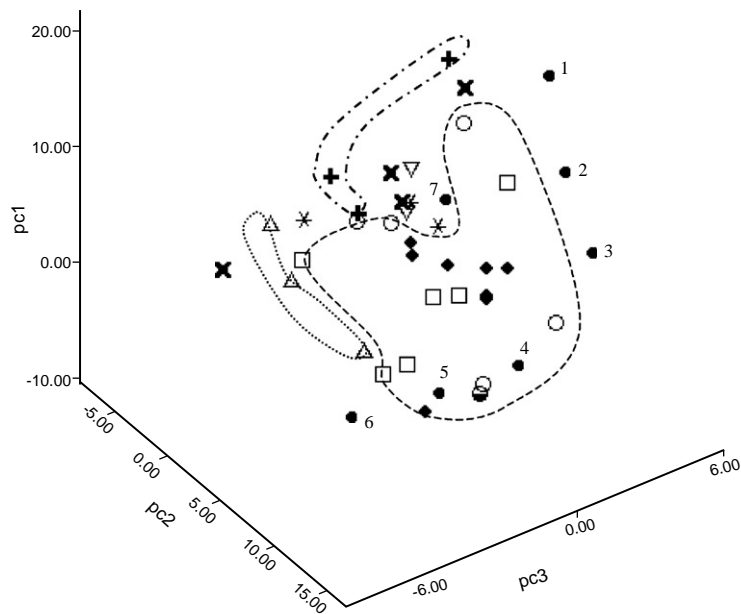


Fig. 1. Principal-component (PC) plot of PC1, PC2 and PC3. (Δ): Lamma Island coal-fired power plant (data encircled by the dotted line); (+): Coastal areas (data encircled by the dash-dotted line); (*): construction sites; (\times): industrial sites; (∇): Lung Kwu Tan coal-fired power plant; (\circ): Covered bus terminals; (\square): Covered car parks. (\blacklozenge): Mong Kok; (\bullet): Causeway Bay; (\ominus): H site; Dashed line: encircling the data points of VE sites, the H site and the two monitoring sites.

In representing the data for our two monitoring sites in a PC plot, it is of interest to find that all data points for the Mong Kok monitoring sites (solid rhombuses in Fig. 1) were located in the area defined by VE reference sites (except one close to the border). We conclude therefore that the main contributor to air pollutants in Mong Kok is vehicular emission.

On the other hand, the data for the Causeway Bay monitoring site suffer more scatter around the VE delineated region. We have sought to explain this scatter in terms of meteorological conditions. The seven data points for the Causeway Bay monitoring site are numbered from 1 to 7 in Fig. 1, and the meteorological data are shown in Table 4. We observe that while points 4 and 5 lie well within the VE area, points 1–3 and 6–7 are positioned outside the area. From the PC plot, points 4 and 5 indicate a vehicular origin to the pollutants, while the main sources of pollutants for points 1–3 and 6–7 are not due to vehicular emissions or due to marine aerosol and coal-fired powered plant.

From Table 4, it is apparent that for relatively high wind speed, the data point will locate outside the VE area (the only exception being CB point 3). This is understandable since vehicular emissions are more easily dispersed while pollutants of other origins can be transported from more distant sources of origin on windy days. Therefore, even at the same place with the

same amount of traffic, a sample that was taken on a day in which higher wind speeds are prevalent may contain relatively smaller amounts of pollutants that are attributable to vehicles. As such, the PC score may deviate from the region defined by vehicles on the principal-component plot. It is particularly interesting to study CB data points numbered 5 and 6, these being recorded on 2 consecutive days. At that time, a cool northeast monsoon reached the coastal areas of Guangdong (during the night of 23 February 2001). As a result, the wind direction changed completely and the mean wind speed increased abruptly. Accordingly, the pollutant composition in the air in Causeway Bay varied, and the data point was displaced from the VE region.

For a reference, the meteorological conditions corresponding to the data points for the Mong Kok monitoring site are also shown in Table 5. Interestingly, again, we see that the data on the border of the VE region corresponds to the largest mean wind speed. Apparently, larger wind speeds would be needed to weaken the contribution of vehicular emissions as the main source of air pollutant in Mong Kok, in comparison to the case of Causeway Bay.

The H site is also a peculiar one, being an industrial area close to a bus stop and two petroleum stations, and surrounded by many tall buildings. During sampling,

Table 4

Some meteorological data for the data points for the Causeway Bay (CB) monitoring site. The CB point numbers refer to the labeled data points in Fig. 1

CB point number	Date	Prevailing wind direction (deg)	Mean wind speed (km/h)	API
1	6 October 2000	090	21.3	72
2	9 February 2001	020	21.2	61
3	19 February 2001	040	14.2	84
4	23 October 2000	090	15.0	72
5	23 February 2001	040	11.4	85
6	24 February 2001	270	24.7	97
7	22 September 2000	070	26.3	76

Table 5

Some meteorological data for the data points for the Mong Kok (MK) monitoring site. The data points are referred to as those positioned either in the interior of or on the border of the VE region in Fig. 1

Position in the VE region in Fig. 1	Date	Prevailing wind direction (deg)	Mean wind speed (km/h)	API
Interior	24 September 2000	100	11.5	49
Border	10 October 2000	080	41.4	N/A
Interior	22 October 2000	120	13.3	N/A
Interior	24 October 2000	030	5.5	N/A
Interior	29 November 2000	070	36.7	N/A
Interior	19 February 2001	040	14.2	90
Interior	24 February 2001	270	24.7	92
Interior	11 March 2001	040	14.5	83

many buses and heavy trucks traversed the sampling location. As the sampling was done 1 m above the ground, it was inconceivable at that height for the air to have a representative mix of industrial and vehicular pollutants, it being more likely that vehicular pollutants dominated the sample. The PC plot in Fig. 1 verified that the main pollutant at this sampling site was indeed vehicular emission.

4. Conclusions

Airborne particulate samples were collected from various reference and monitoring sites in Hong Kong. EDXRF intensities for 19 chemical elements were recorded. PCA was employed so that the variances of these 19 original variables were captured by a few new indices called PCs.

In conclusion, a principal-component plot represents a relatively simple and quick method for identification of the main air pollutants in an area, without recourse to determining the different source profiles beforehand. Thus said, the reliability of the conclusions will depend on the accuracy of the experimental data, the separation of regions defined by different categories of data and the degree of confinement of data for the test sites.

As regards the accuracy of the experimental data, the typical relative uncertainties of the energy dispersive X-ray fluorescence (EDXRF) intensities for different chemical elements are 10–15% in the present study, which should be sufficient to give reliable results. As judged from Fig. 1, regions defined by the different categories of data are well separated. The data for the Mong Kok monitoring site are well confined within the area defined by vehicular emissions, the conclusion being that the main air pollutants originate from vehicular emissions to within high confidence.

Acknowledgements

The present research was supported by research Grant 9030865 from the City University of Hong Kong.

References

- Fung, Y.S., Wong, L.W.Y., 1995. Apportionment of air pollution sources by receptor modeling in Hong Kong. *Atmospheric Environment* 29, 2041–2048.
- Hong Kong Environmental Protection Department (HKEPD), 1997. Air Services Group, Air Quality in Hong Kong 1986–1997 (CD-ROM). The Government of Hong Kong, Hong Kong.
- Kendall, M.G., 1980. *Multivariate Analysis*, 2nd Ed. Griffin, London.
- Lee, E., Chan, C.K., Paatero, P., 1999. Application of positive matrix factorization in source apportionment of particulate pollutants in Hong Kong. *Atmospheric Environment* 33, 3201–3212.
- Manly, B.F.J., 1986. *Multivariate Statistical Methods*. Chapman and Hall, London.
- Orlic, I., 1995. The microanalysis of individual aerosol particles using the nuclear microprobe. *Nucl. Instrum. Methods B* 104, 630–637.
- Stephenson, G., Radmore, P.M., 1990. *Advanced Mathematical Methods for Engineering and Science Students*. Cambridge University Press, Cambridge.
- Yu, K.N., Miao, J.M., 1996. Non-destructive analysis of Jingdezhen blue and white porcelains of the Ming Dynasty using EDXRF. *X-ray Spectrometry* 25, 281–285.
- Yu, K.N., Miao, J.M., 1997. Locating the origins of blue and white porcelains using EDXRF. *Appl. Radiat. Isot.* 48, 959–963.
- Yu, K.N., Yeung, Z.L.L., Lee, L.Y.L., Stokes, M.J., Kwok, R.C.W., 2002. Determination of multi-element profiles of soil using energy dispersive X-ray fluorescence (EDXRF). *Appl. Radiat. Isot.* 57, 279–284.
- Yeung, Z.L.L., Kwok, R.C.W., Yu, K.N., 2003. Determination of multi-element profiles of street dust using Energy Dispersive X-ray Fluorescence (EDXRF). *Appl. Radiat. Isot.* 58, 337–344.